bioRxiv preprint doi: https://doi.org/10.1101/502344; this version posted December 20, 2018. The copyright holder for this preprint (which was not certified by peer review) is the author/funder, who has granted bioRxiv a license to display the preprint in perpetuity. It is made available under aCC-BY 4.0 International license.

Upper bound on the biological effects of 50/60 Hz magnetic fields mediated by radical pairs

P. J. Hore

Department of Chemistry, University of Oxford, Physical & Theoretical Chemistry Laboratory, Oxford OX1 3QZ, UK

peter.hore@chem.ox.ac.uk

Abstract

Prolonged exposure to weak (~1 μT) extremely-low-frequency (ELF, 50/60 Hz) magnetic fields has been associated with an increased risk of childhood leukaemia. One of the few biophysical mechanisms that might account for this link involves short-lived chemical reaction intermediates known as radical pairs. In this report, we use spin dynamics simulations to derive an upper bound of 10 parts per million on the effect of a 1 μT ELF magnetic field on the yield of a radical pair reaction. By comparing this figure with the corresponding effects of changes in the strength of the Earth's magnetic field, we conclude that if exposure to such weak 50/60 Hz magnetic fields has any effect on human biology, and results from a radical pair mechanism, then the risk should be no greater than travelling a few kilometres towards or away from the geomagnetic north or south pole.

1. Introduction

Residents in developed countries are almost continuously exposed to the 50 or 60 Hz electromagnetic fields generated by electrical appliances and power transmission lines. Although these fields are normally very weak in residential environments (electric component < 100 V m^{-1}, magnetic component < 1 μT (1)), these extremely-low-frequency (ELF) fields have been mooted as a potential health hazard (2-4). In relation to childhood leukaemia, ELF magnetic fields have been classified as 'possibly carcinogenic to humans' (5-8). Although there is scant evidence from animal experiments to support a causative link (7, 9), numerous *in vitro* investigations have reported biological effects of ELF fields (reviewed in (10-12)). Not many of these observations have been independently replicated (13). To explain any genuine effects, there must exist biophysical mechanisms by which weak ELF magnetic fields interact with molecules in living organisms. More than 10 years ago, Swanson and Kheifets (1) and Adair (14-16) assessed a range of potential mechanisms and concluded that none was likely to have biological consequences at magnetic flux densities of order 1 μT.

bioRxiv preprint doi: https://doi.org/10.1101/502344; this version posted December 20, 2018. The copyright holder for this preprint (which was not certified by peer review) is the author/funder, who has granted bioRxiv a license to display the preprint in perpetuity. It is made available under aCC-BY 4.0 International license.

One of the mechanisms considered was the radical pair mechanism (4). Unlike some of the others, this is unquestionably a genuine phenomenon supported by hundreds of laboratory studies of (mostly non-biological) chemical reactions in magnetic fields ranging from ~1 mT up to several Tesla (17-22). Radical pairs are short-lived reaction intermediates, typically formed in highly non-equilibrium electron-spin states. Their coherent spin dynamics, combined with spin-dependent reactivity, allow magnetic interactions a million times smaller than the thermal energy, $k_B T$, to have measurable, reproducible and predictable effects on chemical reaction yields. In the last few years, interest in the biological significance of < 1 mT static magnetic fields has been kindled by new insights into the biophysical mechanism of the avian magnetic compass sense (23-27). It now seems likely that migratory songbirds detect the direction of the geomagnetic field by means of photo-induced radical pairs generated within cryptochrome proteins located in their retinas (24, 28, 29). The growing support for this hypothesis includes an experimental demonstration that a radical pair reaction can be influenced by a static magnetic field of the same strength as the geomagnetic field (~50 μT) (30). Whether this hypothesis proves to be correct or not, it is important to distinguish between functional responses, such as magnetoreception, which presumably have been optimised by evolutionary pressure, and fortuitous, non-functional magnetic effects which could in principle be damaging. Since humans seem to navigate without the benefit of in-built magnetic sensors, we focus here exclusively on the latter. However, one cannot exclude the possibility that other biological responses to the Earth's magnetic field, e.g. at the cellular level, could have been useful at an early stage in human evolution and might still persist.

Prompted by their putative role in magnetoreception, cryptochromes have become the focus of recent discussions of fortuitous radical pair effects in biology (31-39). Juutilainen *et al.*, for example, have proposed a hypothesis to explain the link between environmental ELF magnetic fields and childhood leukaemia ('magnetocarcinogenesis') (12). Because cryptochromes are key components of the circadian clock (40-42), and circadian systems are closely coupled to the regulation of DNA damage responses and defence against reactive oxygen species, it is possible that magnetic field effects on radical reactions in cryptochromes could lead to circadian dysregulation, genomic instability and ultimately cancer (12).

Our purpose here is to extend Adair's 1999 discussion (15) of radical pair magnetic field effects by modelling the spin dynamics of cryptochrome-based radical pairs using more advanced theoretical methods. The goal is to derive a realistic order-of-magnitude estimate of the largest likely effect of a 1 μT ELF field in the presence of the Earth's magnetic field. This upper bound is compared with the predicted effects of modest changes in the strength of the geomagnetic field such as would be experienced by travelling around the globe and with the small changes in body temperature that occur naturally in healthy humans.

bioRxiv preprint doi: https://doi.org/10.1101/502344; this version posted December 20, 2018. The copyright holder for this preprint (which was not certified by peer review) is the author/funder, who has granted bioRxiv a license to display the preprint in perpetuity. It is made available under aCC-BY 4.0 International license.

2. Model

2.1 Outline

Our aim is to determine the change in the yield of a radical pair reaction caused by a 1 μT ELF field superimposed on the geomagnetic field. We make no attempt to link this change to any specific biological process; rather we seek to estimate the maximum primary magnetic field effect under chemically and physically plausible conditions. Calculations are based on the [$FAD^{\bullet-}$ $TrpH^{\bullet+}$] radical pair that accounts for the observed effects of static magnetic fields on the photochemistry of purified cryptochromes (24, 43-45). This species is formed by the transfer of an electron from a tryptophan residue (TrpH) in the protein to the photo-excited, non-covalently bound, flavin adenine dinucleotide (FAD) chromophore, Figure 1(a). We consider a simplified spin system comprising the two unpaired electron spins, one on each radical, coupled to three nitrogen nuclei (^{14}N, spin quantum number $I = 1$) chosen for their large isotropic hyperfine coupling constants: N5 and N10 in $FAD^{\bullet-}$ (a = 523 μT and 189 μT) and N1 in $TrpH^{\bullet+}$ (a = 322 μT), calculated using density functional theory (46). The radicals were assumed to have g-values equal to the free electron g-value, 2.0023. At the magnetic field strengths of interest here the difference in the Zeeman interactions of $FAD^{\bullet-}$ and $TrpH^{\bullet+}$ is entirely negligible. We exclude the anisotropic components of the hyperfine interactions which are only relevant when the radicals are immobilized and aligned, as in the case of a magnetic compass sensor (27). These hyperfine interactions condition the response of the radical pair to both static and ELF magnetic fields.

The chemistry of this radical pair was modelled in a simplified fashion by means of competing, spin-selective, singlet and triplet reaction channels (Figure 1(b)). For the present purposes the precise nature of these reactions is immaterial but to avoid unnecessary abstraction we briefly describe the reaction steps in the context of a cryptochrome-based magnetic compass sensor (43). Formed in a spin-correlated singlet state (total electron spin quantum number, $S = 0$), the radical pair coherently interconverts with the corresponding triplet state ($S = 1$) as a result of the internal hyperfine interactions and the Zeeman interactions of the electron spins with any external magnetic fields (24). In cryptochrome, the singlet channel is a reverse electron transfer reaction that returns the charge-separated radical pair state to the diamagnetic ground state of the protein. The triplet channel is considered to produce the signalling state that initiates magnetic signal-transduction (24). For simplicity, the two reaction channels were assigned identical first order rate constants, k (the so-called 'exponential model' (47)). Magnetic field effects arise from the competition between these two spin-conserving reactions together with the change in the extent and timing of the coherent singlet-triplet interconversion brought about by the external magnetic field(s). Although these calculations were performed for a highly simplified model of a radical pair state of cryptochrome, we will argue below (Section 4.2) that general conclusions can be drawn that are relevant to any chemically and physically realistic radical pair reaction.

bioRxiv preprint doi: https://doi.org/10.1101/502344; this version posted December 20, 2018. The copyright holder for this preprint (which was not certified by peer review) is the author/funder, who has granted bioRxiv a license to display the preprint in perpetuity. It is made available under aCC-BY 4.0 International license.

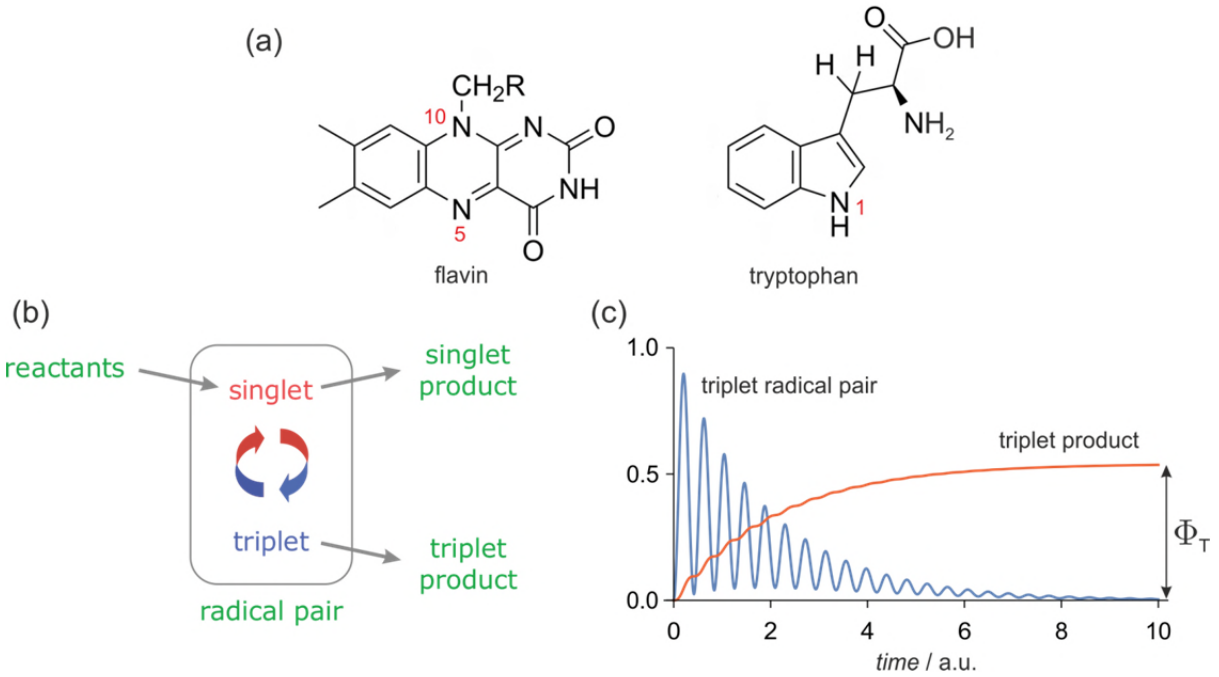

Figure 1. (a) Structures and atom numbers schemes for the FAD and TrpH molecules from which magnetically sensitive radical pairs are formed in purified cryptochromes. (b) Simple reaction scheme for a singlet-born radical pair able to react spin-selectively to form singlet and triplet reaction products. The red/blue arrows represent the coherent interconversion of the two forms of the radical pair. The reaction scheme is a simplified version of the cryptochrome photocycle (24, 43). (c) Schematic dependence of the amounts of triplet radical pair and triplet product present as a function of time (in arbitrary units) after the formation of the radical pair in a singlet state. The triplet yield, Φ_T, is the amount of triplet product formed once all radical pairs have reacted.

Radical pairs can be influenced by magnetic interactions that are minuscule compared to k_BT because they are formed in a spin-coherent state far removed from thermal equilibrium. To be sensitive to a weak static magnetic field, the coherence must persist for a time comparable to the period of the electron Larmor precession which, in a 50 μT magnetic field, is ~700 ns (25). Theoretical treatments often assume negligible spin relaxation during the radical pair lifetime; this is almost always unrealistic (24, 48-50). The reality is that random molecular motions modulate the local magnetic fields experienced by the electron spins causing irreversible loss of spin coherence. Spin relaxation was included here by means of a phenomenological exponential decay towards the equilibrium state (25% singlet, 75% triplet), with a rate constant $r = 10^6$ s^{-1}, corresponding to a spin-coherence lifetime, r^{-1} = 1 μs. This choice of r is discussed in Section 4.2.

Mutual exchange and dipolar interactions of the two unpaired electrons (51) were ignored. The effects of external magnetic fields, both static and time-dependent, were quantified by

bioRxiv preprint doi: https://doi.org/10.1101/502344; this version posted December 20, 2018. The copyright holder for this preprint (which was not certified by peer review) is the author/funder, who has granted bioRxiv a license to display the preprint in perpetuity. It is made available under aCC-BY 4.0 International license.

calculating Φ_T, the fraction of radical pairs that react via the triplet channel ($0 \le \Phi_T \le 1$, Figure 1(c)). We refer to this quantity as the triplet yield. The validity and implications of all the approximations and assumptions involved are discussed in Section 4.2.

2.2 Calculation of Φ_T

In the absence of spin relaxation and chemical reactions, the probability that a radical pair is in a triplet state a time *t* after being created in a singlet state (compare equation (4) of Ref. (47)) is

$$p'_T(t) = 1 - \frac{1}{M}\sum_m \sum_n \left|\langle m|\hat{P}^S|n\rangle\right|^2 \cos\left([\omega_m - \omega_n]t\right), \tag{1}$$

in which $\hbar\omega_i = \langle i|\hat{H}|i\rangle$, where $|i\rangle$ and $\hbar\omega_i$ are, respectively, the eigenstates and eigenvalues of the radical pair spin Hamiltonian, $\hat{H}$, which accounts for the hyperfine and Zeeman interactions of the radicals. $\hat{P}^S$ is the singlet projection operator and *M* is the total number of nuclear spin configurations (47). The oscillatory time-dependence of the triplet probability reflects the formation of the radical pair in a coherent, non-stationary, superposition state.

The spin Hamiltonian of the model [$FAD^{\bullet-}$ $TrpH^{\bullet+}$] radical pair was

$$\hat{H} = \omega\left(\hat{S}_{Az} + \hat{S}_{Bz}\right) + a_1 \hat{\mathbf{S}}_A.\hat{\mathbf{I}}_1 + a_2 \hat{\mathbf{S}}_A.\hat{\mathbf{I}}_2 + a_3 \hat{\mathbf{S}}_B.\hat{\mathbf{I}}_3 \tag{2}$$

with the following spin angular momentum operators: $\hat{\mathbf{S}}_A$ and $\hat{S}_{Az}$, electron in $FAD^{\bullet-}$; $\hat{\mathbf{S}}_B$ and $\hat{S}_{Bz}$, electron in $TrpH^{\bullet+}$ (or $Z^{\bullet}$, see later); $\hat{\mathbf{I}}_1$ and $\hat{\mathbf{I}}_2$ nitrogens N5 and N10 in $FAD^{\bullet-}$; $\hat{\mathbf{I}}_3$, nitrogen N1 in $TrpH^{\bullet+}$. $\omega = \gamma_e B$ is the electron Larmor frequency in a static magnetic field of strength B and a_n ($n = 1-3$) are the hyperfine coupling constants.

Spin relaxation was introduced phenomenologically (compare equation (19) of Ref. (52)) as:

$$p_T(t) = \frac{3}{4} + \left(p'_T(t) - \frac{3}{4}\right)\exp(-rt), \tag{3}$$

where *r* is the relaxation rate constant.

Following Timmel *et al*. (47), the chemical fate of the radical pair was modelled by means of separate spin-selective reactions of the singlet and triplet pairs (Figure 1(b)). To simplify the calculation, these two processes were assigned identical first order rate constants, *k*. The ultimate yield of the product formed spin-selectively from the triplet radical pair state at a time $t \gg k^{-1}$ is therefore:

bioRxiv preprint doi: https://doi.org/10.1101/502344; this version posted December 20, 2018. The copyright holder for this preprint (which was not certified by peer review) is the author/funder, who has granted bioRxiv a license to display the preprint in perpetuity. It is made available under aCC-BY 4.0 International license.

$$\begin{aligned}\Phi_{\mathrm{T}} &= k\int_0^{\infty} p_{\mathrm{T}}(t)\mathrm{e}^{-kt}\,\mathrm{d}t \\ &= \frac{3}{4} + \frac{k}{4(k+r)} - \frac{1}{M}\sum_m\sum_n \left|\langle m|\hat{P}^{\mathrm{S}}|n\rangle\right|^2 \frac{k(k+r)}{(k+r)^2+(\omega_m-\omega_n)^2}.\end{aligned} \tag{4}$$

Equation (4) was used to calculate Φ_{T} and hence mfe_{ELF} and mfe_{GMF} (see below).

2.3 Calculation of mfe_{ELF} and mfe_{GMF}

The same model radical pair was modelled with a weak ELF field superimposed on the geomagnetic field (GMF, B_0 = 50 μT). Epidemiological studies of childhood leukaemia (5, 6, 8) found a two-fold increase in risk for chronic exposure to ELF magnetic fields of root-mean-square magnetic flux density ≥ 0.4 μT with an average strength of ~0.7 μT. The latter corresponds to a peak intensity of $0.7\times\sqrt{2} \approx 1.0$ μT. We therefore take the ELF field to have peak magnetic flux density B_1 = 1.0 μT and frequency 50 Hz. This field is assumed to be linearly polarized and aligned parallel to the GMF such that the total field experienced by the radicals varies between 49 and 51 μT. Any other relative orientation of the two fields would result in a smaller range of total field strengths and smaller ELF effects (see Section 4.2).

Generally requiring lifetimes between 100 ns and 10 μs for a significant LFE (see Section 3.1), magnetically sensitive radical pairs have a fleeting existence compared to the 20 ms period of a 50 Hz electromagnetic wave. Consequently the ELF field can be treated as effectively static during the lifetime of a radical pair (53). We suppose that radical pairs are formed continuously, for example by photo-excitation of cryptochrome. Each radical pair therefore experiences a different, effectively static, magnetic field whose intensity, B, depends on the phase of the ELF field, α, which barely changes during the lifetime of the pair,

$$B = B_0 + B_1\cos\alpha, \tag{5}$$

with α randomly distributed in the range (0, π). The net effect of the ELF field on an ensemble of independently created radical pairs is an average over α,

$$\overline{\Phi_{\mathrm{T}}(B_0,B_1)} = \frac{1}{\pi}\int_0^{\pi}\Phi_{\mathrm{T}}(B)\,\mathrm{d}\alpha. \tag{6}$$

We define the magnetic field effect, mfe_{ELF}, as the relative difference between $\overline{\Phi_{\mathrm{T}}(B_0,B_1)}$ and $\Phi_{\mathrm{T}}(B_0)$, the triplet yield in the absence of the ELF field:

$$mfe_{\mathrm{ELF}} = \frac{\overline{\Phi_{\mathrm{T}}(B_0,B_1)} - \Phi_{\mathrm{T}}(B_0)}{\Phi_{\mathrm{T}}(B_0)}. \tag{7}$$

bioRxiv preprint doi: https://doi.org/10.1101/502344; this version posted December 20, 2018. The copyright holder for this preprint (which was not certified by peer review) is the author/funder, who has granted bioRxiv a license to display the preprint in perpetuity. It is made available under aCC-BY 4.0 International license.

mfe_{ELF} may be evaluated by using $B_1 \ll B_0$ to expand $\Phi_{\mathrm{T}}(B)$ as a Taylor series around $B = B_0$, to second order in $B - B_0$:

$$\Phi_{\mathrm{T}}(B) \approx \Phi_{\mathrm{T}}(B_0) + (B - B_0)\Phi_{\mathrm{T}}^{(1)}(B_0) + \frac{1}{2}(B - B_0)^2 \Phi_{\mathrm{T}}^{(2)}(B_0), \tag{8}$$

where $\Phi_{\mathrm{T}}^{(n)}(B_0)$ is the n-th derivative of $\Phi_{\mathrm{T}}(B)$ evaluated at $B = B_0$. Combining equations (5), (6) and (8) gives the average triplet yield as a sum of zero and second order terms in B_1:

$$\overline{\Phi_{\mathrm{T}}(B_0, B_1)} \approx \Phi_{\mathrm{T}}(B_0) + \frac{1}{4} B_1^2 \Phi_{\mathrm{T}}^{(2)}(B_0). \tag{9}$$

Combining equations (7) and (9) gives:

$$mfe_{\mathrm{ELF}} \approx \frac{1}{4} B_1^2 \frac{\Phi_{\mathrm{T}}^{(2)}(B_0)}{\Phi_{\mathrm{T}}(B_0)}. \tag{10}$$

When $B_1 \ll B_0$, the magnetic field effect, mfe_{ELF}, is thus proportional to the second derivative (i.e. the curvature) of $\Phi_{\mathrm{T}}(B)$ at $B = B_0$ and to the square of the intensity of the ELF field (15, 54).

By analogy with equation (7), we also define a geomagnetic field effect, mfe_{GMF}, as the fractional change in the triplet yield in the absence of an ELF field, when the static magnetic field is changed from B_0 to $B_0 + \Delta B_0$ where $|\Delta B_0| \ll B_0$:

$$mfe_{\mathrm{GMF}} = \frac{\Phi_{\mathrm{T}}(B_0 + \Delta B_0) - \Phi_{\mathrm{T}}(B_0)}{\Phi_{\mathrm{T}}(B_0)}. \tag{11}$$

Expansion of $\Phi_{\mathrm{T}}(B)$ as a Taylor series around $B = B_0$, to first order in ΔB_0, gives

$$mfe_{\mathrm{GMF}} \approx \Delta B_0 \frac{\Phi_{\mathrm{T}}^{(1)}(B_0)}{\Phi_{\mathrm{T}}(B_0)}, \tag{12}$$

which should be compared with equation (10). In contrast to mfe_{ELF}, mfe_{GMF} depends on the *first* derivative (i.e. the gradient) of Φ_{T} and is linear in ΔB_0.

3. Results

3.1 Static magnetic fields

We first look at the dependence of the triplet yield, Φ_{T}, on the strength of an external static magnetic field, B_0, to provide a basis for the discussion of ELF magnetic field effects. Figure 2(a) shows Φ_{T} as a function of B_0 in the range 0–5 mT for seven values of the radical pair lifetime, $\tau = k^{-1}$, between 30 ns and 100 μs. The salient features are as follows. (a) For

bioRxiv preprint doi: https://doi.org/10.1101/502344; this version posted December 20, 2018. The copyright holder for this preprint (which was not certified by peer review) is the author/funder, who has granted bioRxiv a license to display the preprint in perpetuity. It is made available under aCC-BY 4.0 International license.

lifetimes greatly in excess of 1 μs, Φ_T is almost independent of B_0 and approximately equal to 0.75. (b) For intermediate lifetimes ($\tau \approx 1$ μs), the magnetic field effect is bi-phasic: a small increase in Φ_T for $B_0 < 1$ mT is followed by a larger decrease which levels out at fields in excess of 5 mT. The initial 'bump', known as the 'low field effect' (LFE), has been observed in experiments on a variety of radical pair reactions (43, 45, 47, 55, 56). (c) When the lifetime of the radical pair is much shorter than 1 μs, the LFE vanishes and the magnetic field effect becomes mono-phasic. (d) Compared to $B_0 = 0$, a typical geomagnetic field (B_0 = 50 μT) produces the largest change in Φ_T when the LFE is at its most prominent, i.e. for lifetimes, $\tau \approx 1$ μs. This can be seen more clearly in Figure 2(b).

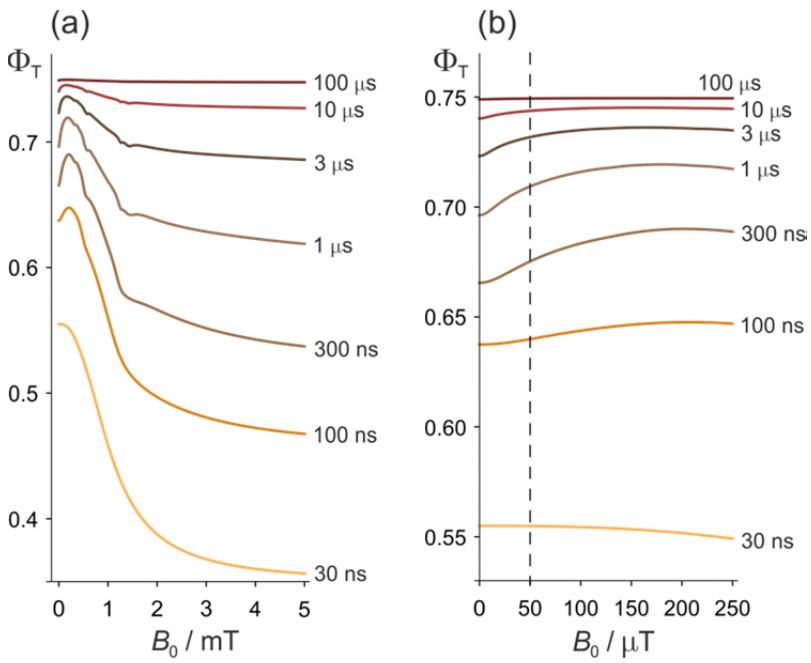

Figure 2. Effects of a static magnetic field on a model of the [FAD$^{\bullet-}$ TrpH$^{\bullet+}$] radical pair in cryptochrome. (a) Dependence of the reaction yield Φ_T on the static magnetic field strength, B_0, for different values of the radical pair lifetime, τ. The spin relaxation time is 1 μs. (b) An expanded view of the low field region of (a) with B_0 = 50 μT indicated by the dashed line. The difference between Φ_T at zero field and at 50 μT is largest when $\tau \approx 1$ μs. The corresponding calculations for a spin relaxation time of 0.1 μs are shown in Figure 2–figure supplement 1.

All the features of Figure 2 that relate to Earth-strength magnetic fields have been observed experimentally and can readily be understood (19, 47). Briefly, if the radical pair exists for much less than 1 μs, there is no time for significant Larmor precession (frequency, 1.4 MHz) in a 50 μT field and hence no additional singlet–triplet interconversion. If the radical pair lives much longer than 1 μs, spin relaxation destroys the spin coherence and establishes a 1:3 singlet:triplet ratio before the radicals can react. In both cases the effect of a 50 μT magnetic

bioRxiv preprint doi: https://doi.org/10.1101/502344; this version posted December 20, 2018. The copyright holder for this preprint (which was not certified by peer review) is the author/funder, who has granted bioRxiv a license to display the preprint in perpetuity. It is made available under aCC-BY 4.0 International license.

field effect is minimal (48-50). The biphasic character of Φ_T arises from two distinct mechanisms: oscillation of low frequency zero-quantum coherences at small B_0 and energetic isolation of two of the three triplet sub-levels at high B_0 (47, 57). The slight irregularities in Φ_T, visible in some of the traces in Figure 2(a), arise from avoided energy-level crossings (58, 59). Such features are usually imperceptible for more realistic spin systems containing a larger number of nuclear spins.

Two other features of Figure 2 will be relevant for our discussion of ELF effects. At $B_0 \approx$ 50 μT, the gradient, $\mathrm{d}\Phi_T / \mathrm{d}B_0$, is positive and the curvature, $\mathrm{d}^2\Phi_T / \mathrm{d}B_0^2$, mostly negative (i.e. concave downward).

3.2 ELF magnetic fields

Before showing simulations of mfe_{ELF}, we anticipate some of its properties. The dependence of mfe_{ELF} on the curvature of Φ_T in equation (10) is rationalised in Figure 3(a) which shows that $mfe_{\mathrm{ELF}} = 0$ if Φ_T depends *linearly* on B in the range $(B_0 - B_1) \le B \le (B_0 + B_1)$. In that case, the average effect of static and ELF fields together (blue arrow) is the same as for the static field alone (green arrow). The change in Φ_T when $0 \le \alpha \le \frac{1}{2}\pi$ exactly cancels that for $\frac{1}{2}\pi \le \alpha \le \pi$. This is not the case when Φ_T has a *non-linear* dependence on B, Figure 3(b).

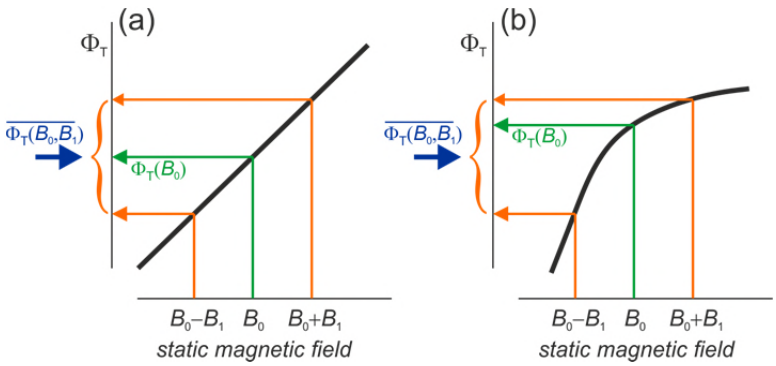

Figure 3. Schematic representations (thick black lines) of the dependence of the reaction yield, Φ_T, on the strength of a static magnetic field. The orange arrows indicate the yields for the maximum and minimum values of B in equation (5). The green arrows show the yields when $B = B_0$. The blue arrows mark the free radical yields averaged over the phase of the ELF field, equation (6). (a) When Φ_T is linear in B, the effect of the GMF and the ELF field *together* equals that of the GMF *alone*. (b) When Φ_T is non-linear, the effects of GMF plus ELF and GMF-alone differ. Φ_T in (b) has been drawn with a negative curvature (concave downward), with the result that $\overline{\Phi_T(B_0,B_1)} < \Phi_T(B_0)$ and $mfe_{\mathrm{ELF}} < 0$ (equations (7) and (10)). A positive curvature (concave upward) would give the opposite signs.

bioRxiv preprint doi: https://doi.org/10.1101/502344; this version posted December 20, 2018. The copyright holder for this preprint (which was not certified by peer review) is the author/funder, who has granted bioRxiv a license to display the preprint in perpetuity. It is made available under aCC-BY 4.0 International license.

From Figures 2 and 3, we can anticipate that for B_0 = 50 μT and B_1 = 1.0 μT, mfe_{ELF} will be largest when the LFE is strongest, i.e. when $\tau \approx 1$ μs. Figure 4(a) shows that this is indeed the case. For lifetimes in the range 1 ns–1 ms, the largest change in the reaction yield caused by the ELF magnetic field is –1.2 parts per million (ppm); mfe_{ELF} is negative because $\Phi^{(2)}(B_0) < 0$ for most values of τ. The significance of the sign of mfe_{ELF} is discussed in Section 4.1.

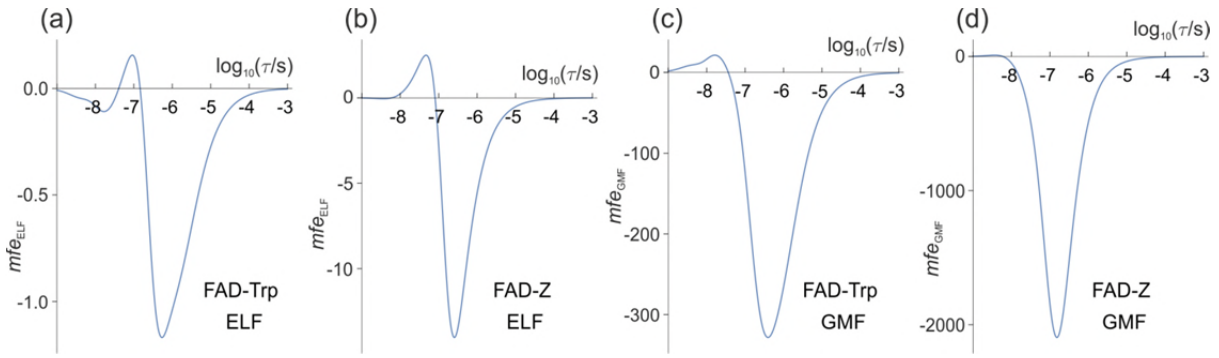

Figure 4. Magnetic field effects (in ppm) on model radical pairs as a function of the lifetime of the radical pair, τ, in the range 1 ns–1 ms. The spin relaxation time is 1 μs. (a) and (c) A model of the [$FAD^{\bullet-}$ $TrpH^{\bullet+}$] radical pair in cryptochrome, containing two ^{14}N nuclei in the $FAD^{\bullet-}$ radical and one in the $TrpH^{\bullet+}$ radical. (b) and (d) A model of the [$FAD^{\bullet-}$ $Z^{\bullet}$] radical pair in cryptochrome in which the $Z^{\bullet}$ radical has no hyperfine interactions. (a) and (b) mfe_{ELF} (equation (10)) for B_0 = 50 μT, B_1 = 1.0 μT. (c) and (d) mfe_{GMF} (equation (12)) for B_0 = 50 μT, ΔB_0 = –1.0 μT. Note the different vertical scales of the four panels. The validity of the Taylor series expansion (equation (9)) was confirmed by numerical integration over α, the phase of the ELF field (Figure 4–figure supplement 1). Corresponding calculations for a spin relaxation time of 0.1 μs are shown in Figure 4–figure supplement 2. Corresponding versions of (a) and (c) when 25 μT $\leq B_0 \leq$ 65 μT are shown in Figure 4–figure supplement 3.

Although magnetic field effects on purified cryptochromes arise from [$FAD^{\bullet-}$ $TrpH^{\bullet+}$], there is some evidence that, *in vivo*, $FAD^{\bullet-}$ is partnered by a radical with fewer, smaller hyperfine interactions than $TrpH^{\bullet+}$ (46, 60). The simulation in Figure 4(a) was therefore repeated for a radical pair, [$FAD^{\bullet-}$ $Z^{\bullet}$], identical to [$FAD^{\bullet-}$ $TrpH^{\bullet+}$] except that the second radical, $Z^{\bullet}$, has no hyperfine interactions. Previous studies, both experimental and theoretical, have shown that such highly asymmetric radical pairs show larger low field effects than when the hyperfine interactions are more evenly distributed between the two radicals (46, 61, 62). As Figure 4(b) shows, this is also the case for ELF fields. The maximum ELF effect for the model [$FAD^{\bullet-}$ $Z^{\bullet}$] pair is –14 ppm, roughly an order of magnitude larger than the largest mfe_{ELF} for [$FAD^{\bullet-}$ $TrpH^{\bullet+}$].

bioRxiv preprint doi: https://doi.org/10.1101/502344; this version posted December 20, 2018. The copyright holder for this preprint (which was not certified by peer review) is the author/funder, who has granted bioRxiv a license to display the preprint in perpetuity. It is made available under aCC-BY 4.0 International license.

3.3 Comparison of ELF and GMF effects

Figures 4(a) and 4(b) suggest that the effect of a 1 μT ELF magnetic field is likely to be no more than a few parts per million. How should such numbers be interpreted in terms of any potential biological significance? The simplest approach would be to assert that changes in the yield of a chemical reaction smaller than, say, 100 ppm (i.e. 0.01%) can be dismissed as insignificant. Although arguably reasonable, the choice of any such threshold is necessarily arbitrary, especially as we have deliberately refrained from considering specific biological processes. An alternative would be to calculate a 'signal-to-noise' ratio in which the 'signal' would be a change in concentration (e.g. of a reactive oxygen species) induced by the ELF field and the 'noise' would be the average background fluctuation in that concentration. Then, with some confidence, one could reject potential ELF effects that had a predicted signal-to-noise ratio less than 1.0. Clearly, this too is unsatisfactory due to lack of knowledge of both the 'noise' and the link between the radical pair reaction and a biological end-point. We have therefore chosen not to rely solely on the absolute values of mfe_{ELF} but instead to compare predicted ELF effects with the changes in Φ_{T} that would arise from small variations in the strength of the geomagnetic field such as might be experienced by moving to a different point on the Earth's surface. Performing the two calculations using the same model and the same parameters allows ELF effects to be put into a more readily appreciated perspective. Furthermore, by taking the ratio of mfe_{ELF} (equation (10)) and mfe_{GMF} (equation (12)) under identical conditions, any errors arising from the approximations and assumptions of the model will tend to cancel.

To facilitate comparison with the ELF effects shown in Figures 4(a) and (b) (for which B_1 = 1.0 μT), we keep B_0 fixed at 50 μT and choose ΔB_0 = –1.0 μT (negative, so that mfe_{GMF} has, for the most part, the same sign as mfe_{ELF}). The results are shown in Figures 4(c) and (d) for the model [$\mathrm{FAD}^{\bullet-}$ $\mathrm{TrpH}^{\bullet+}$] and [$\mathrm{FAD}^{\bullet-}$ $\mathrm{Z}^{\bullet}$] radical pairs respectively. In both cases, the largest mfe_{GMF} exceeds the largest mfe_{ELF} by two orders of magnitude. In the following we denote these maximum magnetic field effects $mfe_{\mathrm{GMF}}^{\max}$ and $mfe_{\mathrm{ELF}}^{\max}$.

Equations (12) and (10) show that mfe_{GMF} and mfe_{ELF} scale, respectively, linearly in ΔB_0 and quadratically in B_1. We can therefore use Figure 4 to predict mfe_{GMF}, mfe_{ELF} and their ratio for different values of ΔB_0 and B_1, provided $|\Delta B_0| \ll B_0$ and $B_1 \ll B_0$. For example, for Figures 4(a) and 4(c), $mfe_{\mathrm{GMF}}^{\max}$ is approximately 280 times larger than $mfe_{\mathrm{ELF}}^{\max}$. mfe_{GMF} and mfe_{ELF} should therefore have similar maximum amplitudes when ΔB_0 is reduced by a factor of 280. Thus, for the model of [$\mathrm{FAD}^{\bullet-}$ $\mathrm{TrpH}^{\bullet+}$], a –3.6 nT change in the geomagnetic field should have roughly the same effect on Φ_{T} as would a 1 μT ELF field. For the simpler [$\mathrm{FAD}^{\bullet-}$ $\mathrm{Z}^{\bullet}$] radical pair (Figures 4(b) and 4(d), where the ratio of $mfe_{\mathrm{GMF}}^{\max}$ to $mfe_{\mathrm{ELF}}^{\max}$ is 150), the corresponding ΔB_0 would be ≈ –6.7 nT.

3.4 Comparison with temperature effects

A different comparison, which may also help to put the predicted ELF effects into context, relates to the daily variation in body temperature which, for a healthy adult, is typically ±0.5 °C. The two parameters in our calculation that are most likely to be temperature-

bioRxiv preprint doi: https://doi.org/10.1101/502344; this version posted December 20, 2018. The copyright holder for this preprint (which was not certified by peer review) is the author/funder, who has granted bioRxiv a license to display the preprint in perpetuity. It is made available under aCC-BY 4.0 International license.

sensitive are the rate constants for the reactions (k) and the relaxation (r) of the radicals. By analogy with equations (10) and (12), we define $Te_{\Delta k,\Delta r}$ (Te = temperature effect) as the change in Φ_{T} resulting from small increases (Δk and Δr) in k and r, respectively,

$$Te_{\Delta k,\Delta r} = \frac{\Phi_{\mathrm{T}}^{(k+\Delta k,r+\Delta r)} - \Phi_{\mathrm{T}}^{(k,r)}}{\Phi_{\mathrm{T}}^{(k,r)}} . \tag{13}$$

To obtain crude estimates of the temperature dependence of Φ_{T}, we assume that both k and r increase/decrease by 0.1% for a temperature rise/fall of 1 °C . Assuming Arrhenius behaviour (rate $\propto \exp[-E_{\mathrm{a}} / RT]$) and T = 37 °C, this corresponds to a small activation energy, E_{a} = 0.80 kJ mol^{-1} ($\approx$ 0.31 RT). Larger activation energies would lead to more dramatic changes in these rate constants.

Taking $k = r = 10^6$ s^{-1}, B_0 = 50 μT and $\Delta B_0 = B_1 = 0$, we find $Te_{\Delta k,0}$ = –36 ppm and $Te_{0,\Delta r}$ = +21 ppm for [FAD$^{\bullet-}$ TrpH$^{\bullet+}$] and $Te_{\Delta k,0}$ = –54 ppm and $Te_{0,\Delta r}$ = +27 ppm for [FAD$^{\bullet-}$ Z$^{\bullet}$]. The two temperature effects are additive: increasing both rate constants by 0.1% simultaneously results in $Te_{\Delta k,\Delta r}$ = –15 ppm for [FAD$^{\bullet-}$ TrpH$^{\bullet+}$] and –27 ppm for [FAD$^{\bullet-}$ Z$^{\bullet}$]. These numbers should be compared with the corresponding values of mfe_{ELF} in Figures 4(a) and (b).

For convenience all the numerical results reported in this Section are collected in Table 1, with $\Omega_{\mathrm{ELF}}^{\mathrm{GMF}}$ defined as the ratio $mfe_{\mathrm{GMF}}^{\max} / mfe_{\mathrm{ELF}}^{\max}$.

bioRxiv preprint doi: https://doi.org/10.1101/502344; this version posted December 20, 2018. The copyright holder for this preprint (which was not certified by peer review) is the author/funder, who has granted bioRxiv a license to display the preprint in perpetuity. It is made available under aCC-BY 4.0 International license.

Table 1. Changes in reaction product yields (in ppm) arising from small changes in magnetic field strengths and temperature

		[FAD$^{\bullet-}$ TrpH$^{\bullet+}$]	[FAD$^{\bullet-}$ Z$^{\bullet}$]
$mfe_{\mathrm{ELF}}^{\max}$ [a]	$B_1 = 1.0\ \mu\mathrm{T}$	−1.2	−14
$mfe_{\mathrm{GMF}}^{\max}$ [a]	$\Delta B_0 = -1.0\ \mu\mathrm{T}$	−330	−2100
$\Omega_{\mathrm{ELF}}^{\mathrm{GMF}}$ [b]		280	150
$Te_{\Delta k,0}$ [c]	$B_1 = \Delta B_0 = 0$	−36	−54
$Te_{0,\Delta r}$ [d]	$B_1 = \Delta B_0 = 0$	+21	+27
$Te_{\Delta k,\Delta r}$ [e]	$B_1 = \Delta B_0 = 0$	−15	−27

[a] $r = 10^6\ \mathrm{s}^{-1}$, $B_0 = 50\ \mu\mathrm{T}$
[b] $\Omega_{\mathrm{ELF}}^{\mathrm{GMF}} = mfe_{\mathrm{GMF}}^{\max} / mfe_{\mathrm{ELF}}^{\max}$
[c] $k = r = 10^6\ \mathrm{s}^{-1}$, $\Delta k = 10^3\ \mathrm{s}^{-1}$, $\Delta r = 0$, $B_0 = 50\ \mu\mathrm{T}$
[d] $k = r = 10^6\ \mathrm{s}^{-1}$, $\Delta k = 0$, $\Delta r = 10^3\ \mathrm{s}^{-1}$, $B_0 = 50\ \mu\mathrm{T}$
[e] $k = r = 10^6\ \mathrm{s}^{-1}$, $\Delta k = \Delta r = 10^3\ \mathrm{s}^{-1}$, $B_0 = 50\ \mu\mathrm{T}$

4. Discussion

4.1 Signs of mfe_{ELF} and mfe_{GMF}

Equations (10) and (12) predict that mfe_{ELF} and mfe_{GMF} depend, respectively, on the curvature and gradient of Φ_{T} at B_0 = 50 μT and Figure 2 shows that these quantities are, respectively, negative and positive for radical pairs that have lifetimes between ~100 ns and 10 μs. Our simulations (Figure 4) bear out this expectation. The presence of a weak ELF field or a small decrease in the strength of the geomagnetic field both reduce the yield of the triplet product and correspondingly increase Φ_{S}, the singlet yield ($\Phi_{\mathrm{S}} + \Phi_{\mathrm{T}} = 1$, Figure 1(b) and (c)). The signs of mfe_{ELF} and mfe_{GMF} are both reversed if the radical pair starts out as a triplet rather than a singlet. Given our wish to be agnostic about the chemical and biological details, it makes no sense to interpret the absolute signs of mfe_{ELF} and mfe_{GMF}.

Nor are the relative signs of mfe_{ELF} and mfe_{GMF} unconditionally useful for interpreting experimental data. Although mfe_{ELF} and mfe_{GMF} have mostly negative values for both radical pairs in Figure 4 (where $r = 10^6\ \mathrm{s}^{-1}$), positive values of both quantities are predicted when $r = 10^7\ \mathrm{s}^{-1}$ (Figure 4–figure supplement 2) as a result of the different dependence of Φ_{T} on B_0 (Figure 2–figure supplement 1).

bioRxiv preprint doi: https://doi.org/10.1101/502344; this version posted December 20, 2018. The copyright holder for this preprint (which was not certified by peer review) is the author/funder, who has granted bioRxiv a license to display the preprint in perpetuity. It is made available under aCC-BY 4.0 International license.

4.2 Assumptions and approximations

Before attempting to draw conclusions from the data in Table 1, we first assess the validity of the assumptions and approximations used to obtain them. The most important of these concern (*a*) spin relaxation, (*b*) hyperfine interactions, (*c*) electron-electron interactions, (*d*) relative motion of the radicals, and (*e*) the ELF field.

(*a*) Spin relaxation of organic radicals at physiological temperatures is likely to be faster than the 1 μs we have assumed here and unlikely to be slower (48). Although one could imagine longer relaxation times (e.g. ~10 μs) in an avian protein (e.g. cryptochrome) optimised for exquisitely sensitive detection of the geomagnetic field, it is highly improbable that these properties could arise by chance. It would require that the random thermal motions of the radicals had very low amplitude or very high frequency or both (24). Neither seems probable in a biological environment at physiological temperatures. If spin relaxation is faster than 1 μs, all magnetic field effects will be smaller than those in Table 1. For example, mfe_{ELF} and mfe_{GMF} are both reduced by roughly an order of magnitude when $r^{-1} = 0.1$ μs, although their ratio is not greatly changed (see Figure 4–figure supplement 2).

(*b*) Organic radicals with the properties needed to show magnetic field effects almost always have more hyperfine interactions than the one or two that have been included here (63). The semi-occupied molecular orbital that contains the unpaired electron in an organic radical is often delocalized so that the electron interacts with several nearby hydrogen and/or nitrogen nuclei. Our experience of spin dynamics simulations has been that the more hyperfine interactions included in both radicals, the smaller the effects of weak magnetic fields. Conversely, the magnetic sensitivity is generally larger when one of the radicals has just a few small hyperfine interactions or none at all (46). As we have seen with [$FAD^{\bullet-}$ $Z^{\bullet}$], removing the single hyperfine interaction from the model $TrpH^{\bullet+}$ radical, increases mfe_{ELF} and mfe_{GMF} by about an order of magnitude (and reduces $\Omega_{\mathrm{ELF}}^{\mathrm{GMF}}$ by a factor of 2, from 280 to 150, Table 1). Biologically relevant radicals with no or very few hydrogen and nitrogen atoms near the unpaired electron are scarce. Superoxide, $O_2^{\bullet-}$, is one and nitric oxide, $NO^{\bullet}$, is another but both have such fast spin relaxation (probably ~1 ns (64, 65)) that they can be excluded (66). The only other radical discussed in the context of magnetoreception is that formed by oxidation of ascorbic acid, $Asc^{\bullet-}$. [$FAD^{\bullet-}$ $Asc^{\bullet-}$] is predicted to show magnetic field effects larger than [$FAD^{\bullet-}$ $TrpH^{\bullet+}$] but smaller than [$FAD^{\bullet-}$ $Z^{\bullet}$] (45, 46, 67). In short, it is difficult to imagine a biologically plausible radical pair whose hyperfine couplings make it significantly more sensitive to weak magnetic fields than the simplified model of [$FAD^{\bullet-}$ $TrpH^{\bullet+}$] we have considered here.

(*c*) In all of the simulations discussed here, we have ignored the possibility that the unpaired electrons in the two radicals have a mutual spin-spin interaction. Although this has been common practice in theoretical treatments of radical pair magnetoreception (24), it only starts to be a good approximation when the exchange and dipolar interactions, which tend to block singlet-triplet interconversion, are smaller than the geomagnetic field (~50 μT). This in turn would require the radicals to be separated by more than 3.8 nm (51). At such large distances,

bioRxiv preprint doi: https://doi.org/10.1101/502344; this version posted December 20, 2018. The copyright holder for this preprint (which was not certified by peer review) is the author/funder, who has granted bioRxiv a license to display the preprint in perpetuity. It is made available under aCC-BY 4.0 International license.

it is extremely doubtful whether spin-selective recombination would be fast enough to compete with spin relaxation. Inclusion of realistic spin-spin interactions can easily attenuate the predicted magnetic field effects by an order of magnitude or more (51).

(*d*) We have treated the radicals as fixed in space partly because that is the case in cryptochrome but more importantly because the effects of weak fields are more pronounced when the radicals are unable to move freely. Translationally diffusing radicals generally show stronger LFEs when their motions are restricted, for example by confinement within a micelle (56, 68, 69). One of the reasons for this is that without such constraints, translational motion is an efficient source of spin relaxation via modulation of exchange interactions (70). Another is that a fraction of the radical pairs inevitably diffuse apart without ever having the opportunity to undergo the spin-selective reaction(s) essential for a magnetic field effect.

(*e*) We have taken the ELF field to be linearly polarized and aligned parallel to the GMF such that the total field experienced by the radicals varies between 49 and 51 μT. Any other choice would result in a smaller range of total field strengths and therefore smaller ELF effects. If a 1 μT ELF field is randomly oriented with respect to a 50 μT static field, then the average total field fluctuates between 49.37 and 50.64 μT, i.e. a variation of ~0.64 μT instead of 1 μT. Given the quadratic dependence on the amplitude of the ELF field (equation (10)), our choice of parallel fields overestimates the ELF effect by a factor of $\sim(0.64)^{-2} \approx 2.4$ compared to random orientations.

To summarize, in all five cases (*a*-*e*) we have deliberately designed the model and chosen its parameters in such a way as to maximize and/or overestimate the sensitivity to weak magnetic fields.

However, as we now discuss, we have also made a few assumptions that could in practice, or at least in principle, cause mfe_{ELF} and/or mfe_{GMF} to exceed the values in Table 1. First we deal with three factors related to the reaction scheme in Figure 1(b). (*f*) Rather than starting as a singlet, the radical pair might be formed in a triplet state or arise from the encounter of radicals with uncorrelated electron spins ('F-pairs') (17, 71). (*g*) The singlet and triplet states of the radical pair could react with different rate constants ('asymmetric recombination') (72). (*h*) Only one of the competing reaction channels needs to be spin-selective: the other can be independent of spin and proceed with identical singlet and triplet rate constants, as is the case for [$FAD^{\bullet-}$ $TrpH^{\bullet+}$] in cryptochrome (43). Simulations of the model [$FAD^{\bullet-}$ $TrpH^{\bullet+}$] radical pair show that relaxing these three assumptions can increase mfe_{ELF} by up to a factor of 5 (73). We stress that these increases in magnetic sensitivity are maxima, corresponding to particular choices of rate constants, initial spin state and reaction scheme. Although evolution could have exploited such conditions, for example to make a more efficient magnetic compass, it seems improbable that they would occur by chance.

(*i*) In calculating the effects of a 1 μT ELF magnetic field we have used a geomagnetic field strength (50 μT) appropriate for northern Europe. Repeating the [$FAD^{\bullet-}$ $TrpH^{\bullet+}$] simulations

bioRxiv preprint doi: https://doi.org/10.1101/502344; this version posted December 20, 2018. The copyright holder for this preprint (which was not certified by peer review) is the author/funder, who has granted bioRxiv a license to display the preprint in perpetuity. It is made available under aCC-BY 4.0 International license.

(Figure 4) with B_0 = 25 μT and 65 μT (the extreme values of the Earth's field) give mfe_{ELF} values respectively 2.2 times bigger and 1.4 times smaller than for B_0 = 50 μT (see Figure 4–figure supplement 3). Similar effects were found for mfe_{GMF} which was 1.4 times bigger when B_0 = 25 μT and 1.2 times smaller when B_0 = 65 μT. We note that Swanson and Kheifets considered whether the Earth's magnetic field could be an 'effect modifier' of the correlation between ELF exposure and incidence of childhood leukaemia (74). They found 'some, but rather limited and not statistically significant, evidence' for this.

Over the years, various mechanisms that could amplify small radical pair magnetic field effects have been suggested, none of which we have so far considered. Four are mentioned here. First (*j*), is the possibility that a superparamagnetic nanoparticle could boost the strength of the ELF field experienced by a nearby radical pair (75). Briefly, the idea is that the 50/60 Hz field could align the instantaneous, fluctuating magnetic moment of the nanoparticle such that the magnetic field close to its surface would be much stronger than the external ELF field but would still oscillate at 50/60 Hz. We can assess the likely importance of this effect using a thermodynamic argument based on ferritin, a naturally occurring superparamagnetic protein, which has an instantaneous magnetic moment, $m \approx 300\mu_B$ (μ_B is the Bohr magneton) (76-78). The energy of the interaction of ferritin with a B_1 = 1 μT magnetic field, $\sim mB_1$, is a million times smaller than the thermal energy, k_BT, at physiological temperature. The alignment of the nanoparticle's magnetic moment, and therefore the amplification of the ELF field, will consequently be negligible.

In the context of cryptochrome-based magnetoreception, two amplification mechanisms have been proposed, and in one case demonstrated experimentally. They rely on (*k*) slow radical termination reactions (45) and (*l*) reactions of the radicals with paramagnetic scavengers (79, 80). Although potentially routes by which evolution could have optimised the sensitivity of a radical pair-based magnetic compass sensor, it seems improbable that such mechanisms would lead to strong amplification by chance.

The final amplification mechanism (*m*) is more speculative (giving, perhaps, greater scope for disproportionate enhancements of ELF magnetic field effects). It requires a reaction scheme involving chemical feedback in which a radical pair is one of the key reaction intermediates (81-87). The inherent non-linearity of such reactions could at least in principle allow small magnetically induced changes in radical pair lifetimes to have a disproportionately large effect on, for example, the amplitude of chemical oscillations. Further, one could imagine an oscillating reaction with a cycle time that coincidentally matched the period of the ELF field which might then be able to 'pump' the oscillations to higher amplitudes. However, this would require some degree of phase-coherence between the ELF field and the biochemical oscillator. Unless there is a mechanism by which an environmental ELF field could *entrain* a biological oscillator, coherent pumping and therefore selective amplification of 50/60 Hz magnetic field effects would seem rather unlikely. It is difficult to think of any mechanism which could explain a specific and disproportionate response of a radical pair reaction to an ELF field.

bioRxiv preprint doi: https://doi.org/10.1101/502344; this version posted December 20, 2018. The copyright holder for this preprint (which was not certified by peer review) is the author/funder, who has granted bioRxiv a license to display the preprint in perpetuity. It is made available under aCC-BY 4.0 International license.

To sum up, we have discussed 13 assumptions and approximations in the simulations on which this article is based. In our judgement, the first five (*a*-*e*) are the most important and almost certainly lead to overestimates of the effects of both ELF and static fields. The next three (*f*-*h*) could, if operating simultaneously, enhance mfe_{ELF} by up to an order of magnitude, but only for specific combinations of rate constants. Using a value other than 50 μT for the Earth's magnetic field (*i*) would increase or decrease mfe_{ELF} and mfe_{GMF}, but only by a factor of ~2. We judge the next three (*j*-*l*) unlikely to have any substantial consequences for biological radical pair reactions that are fortuitously sensitivity to magnetic fields. All of (*a*-*l*) should increase or decrease $mfe_{\mathrm{ELF}}^{\mathrm{max}}$ and $mfe_{\mathrm{GMF}}^{\mathrm{max}}$ to approximately the same degree making their ratio, $\Omega_{\mathrm{ELF}}^{\mathrm{GMF}}$, much less sensitive to the exact conditions of the simulations. Finally, it is difficult to assess the importance of amplification via chemical feedback (*m*) given the highly speculative nature of this mechanism. Certainly, a set of coupled reactions would require some very unusual (and unknown) properties to be able to boost magnetic field effects preferentially at 50/60 Hz. It is not inconceivable that there exists in human biology systems at the cellular level that have evolved sensitivity to the Earth's magnetic field. If so, then some of the above assumptions may be less secure than presented leading to underestimates of magnetic field effects. However, it is still difficult to imagine situations that would selectively enhance responses at 50/60 Hz.

4.3 Additional aspects

Before concluding, we want to mention briefly four additional aspects of radical pair chemistry/physics.

First, when a radical pair is formed in a singlet state, but not when it is formed as an unpolarized triplet, its electron spins are entangled (88). The possibility that entanglement arises naturally in the 'warm, wet and noisy' milieu of a living cell has attracted a certain amount of attention from theoretical physicists (89-94). Nevertheless, there is no apparent way in which this entanglement can enhance magnetic responses (24).

Second, humans have only been exposed to widespread anthropogenic ELF fields since the early days of electrification in the late 19th century. If there is a mechanism by which radical pair reactions can be unusually sensitive to 50/60 Hz magnetic fields, it cannot have evolved in only ~100 years and would have to be a chance consequence of, for example, an unknown cellular response to the Earth's static magnetic field that had evolved at a much earlier stage in human development.

Third, radical pairs are well known to show resonant responses to radiofrequency magnetic fields in the frequency range 1-100 MHz (95-97). Similar effects cannot occur at ELF frequencies because spin relaxation will destroy all spin coherence on a timescale much faster than the 20 ms period of a 50 Hz oscillation. To put it another way: with a ~1 μs coherence lifetime, any resonance would be ~1 MHz wide, thus precluding any possibility that the sensitivity to a 50 Hz field could be greater than that for a static field.

bioRxiv preprint doi: https://doi.org/10.1101/502344; this version posted December 20, 2018. The copyright holder for this preprint (which was not certified by peer review) is the author/funder, who has granted bioRxiv a license to display the preprint in perpetuity. It is made available under aCC-BY 4.0 International license.

Fourth, it appears that radical pairs can only be formed in cryptochromes when the FAD cofactor is correctly bound. Without the flavin, there is very limited scope for the intra-protein electron transfer reactions that could produce magnetically responsive radical pairs. Current evidence suggests that Type 2 vertebrate cryptochromes may be 'vestigial' flavoproteins, unable to bind FAD (98). If true, then human cryptochromes (exclusively Type 2) are unlikely to form radical pairs and therefore improbable as agents of biological radical pair effects. By contrast, Type 4 cryptochromes, which are found in birds, fish and reptiles (99-101), do bind FAD (102-105) and appear to be fit for the purpose as magnetoreceptors in migratory songbirds (106).

5. Conclusions

We believe the values of $mfe_{\mathrm{ELF}}^{\max}$ in Table 1 (–1.2 ppm and –14 ppm for the two model radical pairs considered) provide a good estimate of the maximum fortuitous effect of a 1 μT 50/60 Hz magnetic field on *any* radical pair reaction. Given the arguments in Section 4.2 and the scarcity of biological radicals devoid of significant hyperfine interactions, we propose that 10 ppm should be seen as an upper limit on the change in the yield of a radical pair reaction produced by a 1 μT ELF field in the presence of the Earth's magnetic field (25–65 μT).

To put this number in context, we have estimated the changes in the yields of radical pair reactions that might result from ±0.5 °C variations in temperature. These changes (Table 1) are of the same order of magnitude (~10 ppm) as, or larger than, $mfe_{\mathrm{ELF}}^{\max}$.

Table 1 also contains estimates of the maximum effect ($mfe_{\mathrm{GMF}}^{\max}$) of a 1 μT reduction in the strength of the geomagnetic field in the absence of an ELF field (–330 ppm and –2100 ppm). For similar reasons, we believe these values should also be appropriate for radical pair reactions that have not been optimised for a role in magnetic sensing. The ratios of the two maximum magnetic field effects, $\Omega_{\mathrm{ELF}}^{\mathrm{GMF}} = mfe_{\mathrm{GMF}}^{\max} / mfe_{\mathrm{ELF}}^{\max}$, in Table 1 (280 and 150 for the two model radical pairs) suggest that $\Omega_{\mathrm{ELF}}^{\mathrm{GMF}}$ is likely to be in the range 100–500 for any radical pair reaction. In other words, a 1 μT decrease in the strength of the geomagnetic field should have an effect 100–500 times larger than would a 1 μT ELF field in the presence of the geomagnetic field. Or, equivalently, a 2–10 nT change in the strength of the geomagnetic field should have a similar effect to that of a 1 μT ELF field.

The last result can be put into context by considering the variation in the strength of the geomagnetic field over the surface of the Earth: ~65 μT at the magnetic poles and ~25 μT at the magnetic equator. Given the circumference of the Earth (~40,000 km), the average variation in the geomagnetic field along a line of longitude is roughly 4 nT km^{-1}. Therefore, the maximum effect of a 1 μT ELF field on a radical pair reaction (10 ppm) should be comparable to the maximum effect of travelling 0.5–2.5 km along a north-south axis.

A related comparison, on a much smaller length scale, is provided by measurements of the local distortions in the Earth's magnetic field in homes in the UK caused by the proximity of

bioRxiv preprint doi: https://doi.org/10.1101/502344; this version posted December 20, 2018. The copyright holder for this preprint (which was not certified by peer review) is the author/funder, who has granted bioRxiv a license to display the preprint in perpetuity. It is made available under aCC-BY 4.0 International license.

ferrous objects (107). Variations in static field strength of order 1 μT can be experienced by movement from room to room, corresponding to much larger effects on radical pair reactions than could be expected from a 1 μT ELF field.

It may also be relevant to note that the Earth's magnetic field has a component of amplitude 25–50 nT that oscillates with a 24-hour period (caused by the tidal effect of the sun's gravity on the Earth's atmosphere (108)). Potentially, therefore, the natural diurnal variation in the geomagnetic field could have a larger effect on radical pair chemistry than a 1 μT 50/60 Hz field.

To conclude: the predicted effects of 1 μT ELF magnetic fields in the presence of the Earth's magnetic field are small (< 10 ppm) and similar to or smaller than effects on the same reactions resulting either from travelling a few kilometres or from natural fluctuations in body temperature neither of which would normally be considered as potentially harmful to human health.

Implicit in everything we have written here is the assumption that the current theory of the radical pair mechanism is complete. We cannot exclude the possibility that, despite more than 40 years of research, there is some completely unknown aspect of radical pair spin chemistry that confers a disproportionate sensitivity to ELF magnetic fields. We cannot begin to imagine what that aspect might be except to note a possibly related observation. Migratory birds are prevented from using their magnetic compass by extraordinarily weak broadband radiofrequency noise (60, 109-115) the predicted effects of which are far too small to be consistent with our current understanding of radical pair spin dynamics (116, 117). It is possible, therefore, that a deeper understanding of the mechanism of avian magnetoreception will bring new insights into the risks associated with exposure to weak environmental 50/60 Hz magnetic fields.

Acknowledgements

I am grateful to Jukka Juutilainen, Jim Metcalfe, and John Swanson for helpful comments on the manuscript and to the Electromagnetic Fields Biological Research Trust and its Scientific Advisory Committee for financial support and stimulating discussions over a period of many years.

Competing interests

P. J. Hore declares no competing interests.

Author ORCID

P. J. Hore: http://orcid.org/0000-0002-8863-570X

Author contributions

P. J. Hore did everything.

bioRxiv preprint doi: https://doi.org/10.1101/502344; this version posted December 20, 2018. The copyright holder for this preprint (which was not certified by peer review) is the author/funder, who has granted bioRxiv a license to display the preprint in perpetuity. It is made available under aCC-BY 4.0 International license.

Figure Supplements

Figure 2–figure supplement 1. $\Phi_{\mathrm{T}}\left(B_0\right)$ for $r = 10^7\ \mathrm{s}^{-1}$.

Figure 4–figure supplement 1. $mfe_{\mathrm{ELF}}^{\max}$ evaluated by numerical integration.

Figure 4–figure supplement 2. $mfe_{\mathrm{ELF}}^{\max}$ and $mfe_{\mathrm{GMF}}^{\max}$ for $r = 10^7\ \mathrm{s}^{-1}$.

Figure 4–figure supplement 3. mfe_{ELF} and mfe_{GMF} for $25\ \mu\mathrm{T} \le B_0 \le 65\ \mu\mathrm{T}$.

bioRxiv preprint doi: https://doi.org/10.1101/502344; this version posted December 20, 2018. The copyright holder for this preprint (which was not certified by peer review) is the author/funder, who has granted bioRxiv a license to display the preprint in perpetuity. It is made available under aCC-BY 4.0 International license.

References

1. Swanson, J., and L. Kheifets. 2006. Biophysical mechanisms: a component in the weight of evidence for health effects of power-frequency electric and magnetic fields. *Radiat. Res.* 165:470-478.
2. Crumpton, M. J. 2005. The Bernal Lecture 2004. Are low-frequency electromagnetic fields a health hazard? *Phil. Trans. R. Soc. London B* 360:1223-1230.
3. Crumpton, M. J., and A. R. Collins. 2004. Are environmental electromagnetic fields genotoxic? *DNA Repair* 3:1385-1387.
4. Brocklehurst, B., and K. A. McLauchlan. 1996. Free radical mechanism for the effects of environmental electromagnetic fields on biological systems. *Int. J. Radiat Biol.* 69:3-24.
5. Ahlbom, A., N. Day, M. Feychting, E. Roman, J. Skinner, J. Dockerty, M. Linet, M. McBride, J. Michaelis, J. H. Olsen, T. Tynes, and P. K. Verkasalo. 2000. A pooled analysis of magnetic fields and childhood leukaemia. *Brit J Cancer* 83:692-698.
6. Greenland, S., A. R. Sheppard, W. T. Kaune, C. Poole, and M. A. Kelsh. 2000. A pooled analysis of magnetic fields, wire codes, and childhood leukemia. *Epidemiology* 11:624-634.
7. IARC. 2002. Static and extremely low-frequency (ELF) electric and magnetic fields, vol. 80. Lyon, France: International Agency for Research on Cancer.
8. Kheifets, L., A. Ahlbom, C. M. Crespi, G. Draper, J. Hagihara, R. M. Lowenthal, G. Mezei, S. Oksuzyan, J. Schuz, J. Swanson, A. Tittarelli, M. Vinceti, and V. Wunsch. 2010. Pooled analysis of recent studies on magnetic fields and childhood leukaemia. *Brit J Cancer* 103:1128-1135.
9. WHO. 2007. Extremely low frequency fields. Geneva, Switzerland: World Health Organization.
10. Juutilainen, J., T. Kumlin, and J. Naarala. 2006. Do extremely low frequency magnetic fields enhance the effects of environmental carcinogens? A meta-analysis of experimental studies. *Int. J. Radiat Biol.* 82:1-12.
11. Mattsson, M. O., and M. Simko. 2014. Grouping of experimental conditions as an approach to evaluate effects of extremely low-frequency magnetic fields on oxidative response in *in vitro* studies. *Front. Public Health* 2:132.
12. Juutilainen, J., M. Herrala, J. Luukkonen, J. Naarala, and P. J. Hore. 2018. Magnetocarcinogenesis: is there a mechanism for carcinogenic effects of weak magnetic fields? *Proc. R. Soc. B* 285:20180590.
13. Lacy-Hulbert, A., J. C. Metcalfe, and R. Hesketh. 1998. Biological responses to electromagnetic fields. *FASEB J.* 12:395-420.
14. Adair, R. K. 1991. Constraints on biological effects of weak extremely-low-frequency electromagnetic-fields. *Phys. Rev. A* 43:1039-1048.
15. Adair, R. K. 1999. Effects of very weak magnetic fields on radical pair reformation. *Bioelectromagnetics* 20:255-263.
16. Adair, R. K. 2000. Static and low-frequency magnetic field effects: health risks and therapies. *Rep. Prog. Phys.* 63:415–454.
17. Steiner, U. E., and T. Ulrich. 1989. Magnetic field effects in chemical kinetics and related phenomena. *Chem. Rev.* 89:51-147.
18. Brocklehurst, B. 2002. Magnetic fields and radical reactions: recent developments and their role in Nature. *Chem. Soc. Rev.* 31:301-311.
19. Rodgers, C. T. 2009. Magnetic field effects in chemical systems. *Pure Appl. Chem.* 81:19-43.
20. Jones, A. R. 2016. Magnetic field effects in proteins. *Molec. Phys.* 114:1691-1702.
21. Hore, P. J. 2012. Are biochemical reactions affected by weak magnetic fields? *Proc. Natl. Acad. Sci. USA* 109:1357-1358.
22. Scaiano, J. C., F. L. Cozens, and J. Mclean. 1994. Model for the rationalization of magnetic field effects *in vivo*. Application of the radical pair mechanism to biological systems. *Photochem. Photobiol.* 59:585-589.

bioRxiv preprint doi: https://doi.org/10.1101/502344; this version posted December 20, 2018. The copyright holder for this preprint (which was not certified by peer review) is the author/funder, who has granted bioRxiv a license to display the preprint in perpetuity. It is made available under aCC-BY 4.0 International license.

23. Mouritsen, H. 2018. Long-distance navigation and magnetoreception in migratory animals. *Nature* 558:50-59.
24. Hore, P. J., and H. Mouritsen. 2016. The radical pair mechanism of magnetoreception. *Annu. Rev. Biophys.* 45:299-344.
25. Rodgers, C. T., and P. J. Hore. 2009. Chemical magnetoreception in birds: a radical pair mechanism. *Proc. Natl. Acad. Sci. USA* 106:353-360.
26. Nordmann, G. C., T. Hochstoeger, and D. A. Keays. 2017. Magnetoreception - a sense without a receptor. *PLoS Biol.* 15:e2003234.
27. Schulten, K., C. E. Swenberg, and A. Weller. 1978. A biomagnetic sensory mechanism based on magnetic field modulated coherent electron spin motion. *Z. Phys. Chem. NF* 111:1-5.
28. Ritz, T., S. Adem, and K. Schulten. 2000. A model for photoreceptor-based magnetoreception in birds. *Biophys. J.* 78:707-718.
29. Liedvogel, M., and H. Mouritsen. 2010. Cryptochromes—a potential magnetoreceptor: what do we know and what do we want to know? *J. R. Soc. Interface* 7:S147-S162.
30. Maeda, K., K. B. Henbest, F. Cintolesi, I. Kuprov, C. T. Rodgers, P. A. Liddell, D. Gust, C. R. Timmel, and P. J. Hore. 2008. Chemical compass model of avian magnetoreception. *Nature* 453:387-390.
31. Bounds, P. L., and N. Kuster. 2015. Is cryptochrome a primary sensor of extremely low frequency magnetic fields in childhood leukemia? *Biophys. J.* 108:562a-562a.
32. Lagroye, I., Y. Percherancier, J. Juutilainen, F. Poulletier De Gannes, and B. Veyret. 2011. ELF magnetic fields: animal studies, mechanisms of action. *Prog. Biophys. Molec. Biol.* 107:369-373.
33. Vanderstraeten, J., H. Burda, L. Verschaeve, and C. De Brouwer. 2015. Could magnetic fields affect the circadian clock function of cryptochromes? Testing the basic premise of the cryptochrome hypothesis (ELF magnetic fields). *Health Phys.* 109:84-89.
34. Close, J. 2012. Are stress responses to geomagnetic storms mediated by the cryptochrome compass system? *Proc. R. Soc. B* 279:2081-2090.
35. Close, J. P. 2014. The compass within the clock - Part 1: The hypothesis of magnetic fields as secondary zeitgebers to the circadian system—logical and scientific objections. *Hypothesis* 12:e1.
36. Close, J. P. 2014. The compass within the clock - Part 2: Does cryptochrome radical-pair based signalling contribute to the temperature-robustness of circadian systems? *Hypothesis* 12:e2.
37. Landler, L., and D. A. Keays. 2018. Cryptochrome: the magnetosensor with a sinister side? *PLoS Biol.* 16:e3000018.
38. Krylov, V. V. 2017. Biological effects related to geomagnetic activity and possible mechanisms. *Bioelectromagnetics* 38:497-510.
39. Agliassa, C., R. Narayana, J. M. Christie, and M. E. Maffei. 2018. Geomagnetic field impacts on cryptochrome and phytochrome signaling. *J. Photochem. Photobiol. B* 185:32-40.
40. Chaves, I., R. Pokorny, M. Byrdin, N. Hoang, T. Ritz, K. Brettel, L. O. Essen, G. T. J. van der Horst, A. Batschauer, and M. Ahmad. 2011. The cryptochromes: blue light photoreceptors in plants and animals. *Ann. Rev. Plant Biol.* 62:335-364.
41. Kelleher, F. C., A. Rao, and A. Maguire. 2014. Circadian molecular clocks and cancer. *Cancer Lett.* 342:9-18.
42. Hastings, M. H., M. Brancaccio, and E. S. Maywood. 2014. Circadian pacemaking in cells and circuits of the suprachiasmatic nucleus. *J. Neuroendocrinol.* 26:2-10.
43. Maeda, K., A. J. Robinson, K. B. Henbest, H. J. Hogben, T. Biskup, M. Ahmad, E. Schleicher, S. Weber, C. R. Timmel, and P. J. Hore. 2012. Magnetically sensitive light-induced reactions in cryptochrome are consistent with its proposed role as a magnetoreceptor. *Proc. Natl. Acad. Sci. USA* 109:4774-4779.
44. Sheppard, D. M. W., J. Li, K. B. Henbest, S. R. T. Neil, K. Maeda, J. Storey, E. Schleicher, T. Biskup, R. Rodriguez, S. Weber, P. J. Hore, C. R. Timmel, and S. R. Mackenzie. 2017. Millitesla magnetic field effects on the photocycle of *Drosophila melanogaster* cryptochrome. *Sci. Rep.* 7:42228.

bioRxiv preprint doi: https://doi.org/10.1101/502344; this version posted December 20, 2018. The copyright holder for this preprint (which was not certified by peer review) is the author/funder, who has granted bioRxiv a license to display the preprint in perpetuity. It is made available under aCC-BY 4.0 International license.

45. Kattnig, D. R., E. W. Evans, V. Déjean, C. A. Dodson, M. I. Wallace, S. R. Mackenzie, C. R. Timmel, and P. J. Hore. 2016. Chemical amplification of magnetic field effects relevant to avian magnetoreception. *Nat. Chem.* 8:384-391.
46. Lee, A. A., J. C. S. Lau, H. J. Hogben, T. Biskup, D. R. Kattnig, and P. J. Hore. 2014. Alternative radical pairs for cryptochrome-based magnetoreception. *J. R. Soc. Interface* 11:20131063.
47. Timmel, C. R., U. Till, B. Brocklehurst, K. A. McLauchlan, and P. J. Hore. 1998. Effects of weak magnetic fields on free radical recombination reactions. *Molec. Phys.* 95:71-89.
48. Kattnig, D. R., I. A. Solov'yov, and P. J. Hore. 2016. Electron spin relaxation in cryptochrome-based magnetoreception. *Phys. Chem. Chem. Phys.* 18:12443-12456.
49. Kattnig, D. R., J. K. Sowa, I. A. Solov'yov, and P. J. Hore. 2016. Electron spin relaxation can enhance the performance of a cryptochrome-based magnetic compass sensor. *New J. Phys.* 18:063007.
50. Worster, S., D. R. Kattnig, and P. J. Hore. 2016. Spin relaxation of radicals in cryptochrome and its role in avian magnetoreception. *J. Chem. Phys.* 145:035104.
51. Efimova, O., and P. J. Hore. 2008. Role of exchange and dipolar interactions in the radical pair model of the avian magnetic compass. *Biophys. J.* 94:1565-1574.
52. Bagryansky, V. A., V. I. Borovkov, and Y. N. Molin. 2007. Quantum beats in radical pairs. *Russ. Chem. Rev.* 76:493-506.
53. Scaiano, J. C., N. Mohtat, F. L. Cozens, J. Mclean, and A. Thansandote. 1994. Application of the radical pair mechanism to free radicals in organized systems: can the effects of 60 Hz be predicted from studies under static fields? *Bioelectromagnetics* 15:549-554.
54. Adair, R. K. 1994. Biological responses to weak 60-Hz electric and magnetic-fields must vary as the square of the field-strength. *Proc. Natl. Acad. Sci. USA* 91:9422-9425.
55. Brocklehurst, B. 1976. Spin correlation in geminate recombination of radical ions in hydrocarbons. 1. Theory of magnetic-field effect. *J. Chem. Soc. Faraday Trans. II* 72:1869-1884.
56. Eveson, R. W., C. R. Timmel, B. Brocklehurst, P. J. Hore, and K. A. McLauchlan. 2000. The effects of weak magnetic fields on radical recombination reactions in micelles. *Internat. J. Radiat. Biol.* 76:1509-1522.
57. Till, U., C. R. Timmel, B. Brocklehurst, and P. J. Hore. 1998. The influence of very small magnetic fields on radical recombination reactions in the limit of slow recombination. *Chem. Phys. Lett.* 298:7-14.
58. Timmel, C. R., F. Cintolesi, B. Brocklehurst, and P. J. Hore. 2001. Model calculations of magnetic field effects on the recombination reactions of radicals with anisotropic hyperfine interactions. *Chem. Phys. Lett.* 334:387-395.
59. Hiscock, H. G., S. Worster, D. R. Kattnig, C. Steers, Y. Jin, D. E. Manolopoulos, H. Mouritsen, and P. J. Hore. 2016. The quantum needle of the avian magnetic compass. *Proc. Natl. Acad. Sci. USA* 113:4634-4639.
60. Ritz, T., R. Wiltschko, P. J. Hore, C. T. Rodgers, K. Stapput, P. Thalau, C. R. Timmel, and W. Wiltschko. 2009. Magnetic compass of birds is based on a molecule with optimal directional sensitivity. *Biophys. J.* 96:3451-3457.
61. Stass, D. V., N. N. Lukzen, B. M. Tadjikov, and Y. N. Molin. 1995. Manifestation of quantum coherence upon recombination of radical-ion pairs in weak magnetic fields - systems with nonequivalent nuclei. *Chem. Phys. Lett.* 233:444-450.
62. Rodgers, C. T., S. A. Norman, K. B. Henbest, C. R. Timmel, and P. J. Hore. 2007. Determination of radical re-encounter probability distributions from magnetic field effects on reaction yields. *J. Amer. Chem. Soc.* 129:6746-6755.
63. Gerson, F., and W. Huber. 2003. Electron spin resonance spectroscopy of organic radicals. Wiley-VCH, Weinheim.
64. Karogodina, T. Y., S. V. Sergeeva, and D. V. Stass. 2009. Magnetic field effect in the reaction of recombination of nitric oxide and superoxide anion. *Appl. Magn. Reson.* 36:195-208.

bioRxiv preprint doi: https://doi.org/10.1101/502344; this version posted December 20, 2018. The copyright holder for this preprint (which was not certified by peer review) is the author/funder, who has granted bioRxiv a license to display the preprint in perpetuity. It is made available under aCC-BY 4.0 International license.

65. Karogodina, T. Y., I. G. Dranov, S. V. Sergeeva, D. V. Stass, and U. E. Steiner. 2011. Kinetic magnetic-field effect involving the small biologically relevant inorganic radicals nitric oxide and superoxide. *Chem. Phys. Chem.* 12:1714-1728.
66. Hogben, H. J., O. Efimova, N. Wagner-Rundell, C. R. Timmel, and P. J. Hore. 2009. Possible involvement of superoxide and dioxygen with cryptochrome in avian magnetoreception: origin of Zeeman resonances observed by *in vivo* EPR spectroscopy. *Chem. Phys. Lett.* 480:118-122.
67. Nielsen, C., D. R. Kattnig, E. Sjulstok, P. J. Hore, and I. A. Solov'yov. 2017. Ascorbic acid may not be involved in cryptochrome-based magnetoreception. *J. R. Soc. Interface* 14:20170657.
68. Turro, N. J., and G. C. Weed. 1983. Micellar systems as supercages for reactions of geminate radical pairs - magnetic effects. *J. Amer. Chem. Soc.* 105:1861-1868.
69. Sakaguchi, Y., and H. Hayashi. 1984. Laser-photolysis study of the photochemical-reactions of naphthoquinones in a sodium dodecyl-sulfate micelle under high magnetic-fields. *J. Phys. Chem.* 88:1437-1440.
70. Shushin, A. I. 1991. The effect of the spin exchange interaction on SNP and RYDMR spectra of geminate radical pairs. *Chem. Phys. Lett.* 181:274-278.
71. Salikhov, K. M., Y. N. Molin, R. Z. Sagdeev, and A. L. Buchachenko. 1984. Spin polarization and magnetic field effects in radical reactions. Elsevier, New York.
72. Lewis, A. M., D. E. Manolopoulos, and P. J. Hore. 2014. Asymmetric recombination and electron spin relaxation in the semiclassical theory of radical pair reactions. *J. Chem. Phys.* 141:044111.
73. Blunsden, J. 2018. Effects of weak magnetic fields on radical pair reactions. Part II thesis, University of Oxford.
74. Swanson, J., and L. Kheifets. 2012. Could the geomagnetic field be an effect modifier for studies of power-frequency magnetic fields and childhood leukaemia? *J. Radiol. Prot.* 32:413-418.
75. Binhi, V. 2008. Do naturally occurring magnetic nanoparticles in the human body mediate increased risk of childhood leukaemia with EMF exposure? *Int. J. Radiat. Biol.* 84:569-579.
76. Kilcoyne, S. H., and R. Cywinski. 1995. Ferritin - a model superparamagnet. *J. Magn. Magn. Mater.* 140:1466-1467.
77. Vohralik, P. F., and S. K. H. Lam. 2009. NanoSQUID detection of magnetization from ferritin nanoparticles. *Supercon. Sci. Technol.* 22:64007.
78. Worster, S. B., and P. J. Hore. 2018. Proposal to use superparamagnetic nanoparticles to test the role of cryptochrome in magnetoreception. *J. R. Soc. Interface* 15:20180587.
79. Kattnig, D. R., and P. J. Hore. 2017. The sensitivity of a radical pair compass magnetoreceptor can be significantly amplified by radical scavengers. *Sci. Rep.* 7:11640.
80. Kattnig, D. R. 2017. Radical-pair-based magnetoreception amplified by radical scavenging: resilience to spin relaxation. *J. Phys. Chem. B* 121:10215-10227.
81. Eichwald, C., and J. Walleczek. 1996. Model for magnetic field effects on radical pair recombination in enzyme kinetics. *Biophys. J.* 71:623-631.
82. Eichwald, C., and J. Walleczek. 1997. Low-frequency-dependent effects of oscillating magnetic fields on radical pair recombination in enzyme kinetics. *J. Chem. Phys.* 107:4943-4950.
83. Eichwald, C., and J. Walleczek. 1998. Magnetic field perturbations as a tool for controlling enzyme-regulated and oscillatory biochemical reactions. *Biophys. Chem.* 74:209-224.
84. Møller, A. C., and L. F. Olsen. 1999. Effect of magnetic fields on an oscillating enzyme reaction. *J. Am. Chem. Soc.* 121:6351-6354.
85. Møller, A. C., A. Lunding, and L. F. Olsen. 2000. Further studies of the effect of magnetic fields on the oscillating peroxidase-oxidase reaction. *Phys. Chem. Chem. Phys.* 2:3443-3446.
86. Møller, A. C., and L. F. Olsen. 2000. Perturbations of simple oscillations and complex dynamics in the peroxidase-oxidase reaction using magnetic fields. *J. Phys. Chem. B* 104:140-146.

bioRxiv preprint doi: https://doi.org/10.1101/502344; this version posted December 20, 2018. The copyright holder for this preprint (which was not certified by peer review) is the author/funder, who has granted bioRxiv a license to display the preprint in perpetuity. It is made available under aCC-BY 4.0 International license.

87. Purtov, P. A. 2004. External magnetic fields as a possible cause of stability disturbance of stationary states far from equilibrium in reactions involving radical pairs. *Appl. Magn. Reson.* 26:83-97.
88. Hogben, H. J., T. Biskup, and P. J. Hore. 2012. Entanglement and sources of magnetic anisotropy in radical pair-based avian magnetoreceptors. *Phys. Rev. Lett.* 109:220501.
89. Cai, J., G. G. Guerreschi, and H. J. Briegel. 2010. Quantum control and entanglement in a chemical compass. *Phys. Rev. Lett.* 104:220502.
90. Gauger, E. M., E. Rieper, J. J. L. Morton, S. C. Benjamin, and V. Vedral. 2011. Sustained quantum coherence and entanglement in the avian compass. *Phys. Rev. Lett.* 106:040503.
91. Kominis, I. K. 2012. Magnetic sensitivity and entanglement dynamics of the chemical compass. *Chem. Phys. Lett.* 542:143-146.
92. Pauls, J. A., Y. T. Zhang, G. P. Berman, and S. Kais. 2013. Quantum coherence and entanglement in the avian compass. *Phys. Rev. E* 87:062704.
93. Tiersch, M., G. G. Guerreschi, J. Clausen, and H. J. Briegel. 2014. Approaches to measuring entanglement in chemical magnetometers. *J. Phys. Chem. A* 118:13-20.
94. Zhang, Y. T., G. P. Berman, and S. Kais. 2014. Sensitivity and entanglement in the avian chemical compass. *Phys. Rev. E* 90:042707.
95. Henbest, K. B., P. Kukura, C. T. Rodgers, P. J. Hore, and C. R. Timmel. 2004. Radio frequency magnetic field effects on a radical recombination reaction: a diagnostic test for the radical pair mechanism. *J. Amer. Chem. Soc.* 126:8102-8103.
96. Frankevich, E. L., and S. I. Kubarev. 1982. Spectroscopy of reaction yield detected magnetic resonance. In Triplet state ODMR spectroscopy. R. H. Clarke, editor. Wiley, New York. 137-183.
97. Woodward, J. R., C. R. Timmel, K. A. McLauchlan, and P. J. Hore. 2001. Radio frequency magnetic field effects on electron-hole recombination. *Phys. Rev. Lett.* 87:077602.
98. Kutta, R. J., N. Archipowa, L. O. Johannissen, A. R. Jones, and N. S. Scrutton. 2017. Vertebrate cryptochromes are vestigial flavoproteins. *Sci. Rep.* 7:44906.
99. Kobayashi, Y., T. Ishikawa, J. Hirayama, H. Daiyasu, S. Kanai, H. Toh, I. Fukuda, T. Tsujimura, N. Terada, Y. Kamei, S. Yuba, S. Iwai, and T. Todo. 2000. Molecular analysis of zebrafish photolyase/cryptochrome family: two types of cryptochromes present in zebrafish. *Genes Cells* 5:725-738.
100. Kubo, Y., M. Akiyama, Y. Fukada, and T. Okano. 2006. Molecular cloning, mRNA expression, and immunocytochemical localization of a putative blue-light photoreceptor CRY4 in the chicken pineal gland. *J. Neurochem.* 97:1155-1165.
101. Kubo, Y., T. Takeuchi, K. Okano, and T. Okano. 2010. Cryptochrome genes are highly expressed in the ovary of the african clawed frog, *Xenopus tropicalis*. *Plos One* 5:e9273.
102. Ozturk, N., C. P. Selby, S. H. Song, R. Ye, C. Tan, Y. T. Kao, D. P. Zhong, and A. Sancar. 2009. Comparative photochemistry of animal Type 1 and Type 4 cryptochromes. *Biochemistry* 48:8585-8593.
103. Mitsui, H., T. Maeda, C. Yamaguchi, Y. Tsuji, R. Watari, Y. Kubo, K. Okano, and T. Okano. 2015. Overexpression in yeast, photocycle, and in vitro structural change of an avian putative magnetoreceptor cryptochrome 4. *Biochemistry* 54:1908-1917.
104. Qin, S., H. Yin, C. Yang, Y. Dou, Z. Liu, P. Zhang, H. Yu, Y. Huang, J. Feng, J. Hao, J. Hao, L. Deng, X. Yan, X. Dong, Z. Zhao, T. Jiang, H.-W. Wang, S.-J. Luo, and C. Xie. 2016. A magnetic protein biocompass. *Nat. Mater.* 15:217-226.
105. Wang, X., C. Jing, C. P. Selby, Y.-Y. Chiou, Y. Yang, W. J. Wu, A. Sancar, and J. Wang. 2018. Comparative properties and functions of type 2 and type 4 pigeon cryptochromes. *Cell. Molec. Life Sci.* 75:4629-4641.
106. Günther, A., A. Einwich, E. Sjulstok, R. Feederle, P. Bolte, K. W. Koch, I. A. Solov'yov, and H. Mouritsen. 2018. Double-cone localization and seasonal expression pattern suggest a role in magnetoreception for European robin cryptochrome 4. *Curr. Biol.* 28:211-223.
107. Swanson, J. 1994. Measurements of static magnetic fields in homes in the UK and their implication for epidemiological studies of exposure to alternating magnetic fields. *J. Radiol. Prot.* 14:67-75.

bioRxiv preprint doi: https://doi.org/10.1101/502344; this version posted December 20, 2018. The copyright holder for this preprint (which was not certified by peer review) is the author/funder, who has granted bioRxiv a license to display the preprint in perpetuity. It is made available under aCC-BY 4.0 International license.

108. Liboff, A. R. 2014. Why are living things sensitive to weak magnetic fields? *Electromagn. Biol. Med.* 33:241-245.
109. Ritz, T., P. Thalau, J. B. Phillips, R. Wiltschko, and W. Wiltschko. 2004. Resonance effects indicate a radical-pair mechanism for avian magnetic compass. *Nature* 429:177-180.
110. Thalau, P., T. Ritz, K. Stapput, R. Wiltschko, and W. Wiltschko. 2005. Magnetic compass orientation of migratory birds in the presence of a 1.315 MHz oscillating field. *Naturwissenschaften* 92:86-90.
111. Winklhofer, M., E. Dylda, P. Thalau, W. Wiltschko, and R. Wiltschko. 2013. Avian magnetic compass can be tuned to anomalously low magnetic intensities. *Proc. R. Soc. B* 280:20130853.
112. Engels, S., N. L. Schneider, N. Lefeldt, C. M. Hein, M. Zapka, A. Michalik, D. Elbers, A. Kittel, P. J. Hore, and H. Mouritsen. 2014. Anthropogenic electromagnetic noise disrupts magnetic compass orientation in a migratory bird. *Nature* 509:353-356.
113. Kavokin, K., N. Chernetsov, A. Pakhomov, J. Bojarinova, D. Kobylkov, and B. Namozov. 2014. Magnetic orientation of garden warblers (*Sylvia borin*) under 1.4 MHz radiofrequency magnetic field. *J. R. Soc. Interface* 11:20140451.
114. Wiltschko, R., P. Thalau, D. Gehring, C. Niessner, T. Ritz, and W. Wiltschko. 2015. Magnetoreception in birds: the effect of radio-frequency fields. *J. R. Soc. Interface* 12:20141103.
115. Schwarze, S., N.-L. Schneider, T. Reichl, D. Dreyer, N. Lefeldt, S. Engels, N. Baker, P. J. Hore, and H. Mouritsen. 2016. Weak broadband electromagnetic fields are more disruptive to magnetic compass orientation in a night-migratory songbird (*Erithacus rubecula*) than strong narrow-band fields. *Front. Behav. Neurosci.* 10:55.
116. Kavokin, K. V. 2009. The puzzle of magnetic resonance effect on the magnetic compass of migratory birds. *Bioelectromagnetics* 30:402-410.
117. Hiscock, H. G., H. Mouritsen, D. E. Manolopoulos, and P. J. Hore. 2017. Disruption of magnetic compass orientation in migratory birds by radiofrequency electromagnetic fields. *Biophys. J.* 113:1475-1484.

bioRxiv preprint doi: https://doi.org/10.1101/502344; this version posted December 20, 2018. The copyright holder for this preprint (which was not certified by peer review) is the author/funder, who has granted bioRxiv a license to display the preprint in perpetuity. It is made available under aCC-BY 4.0 International license.

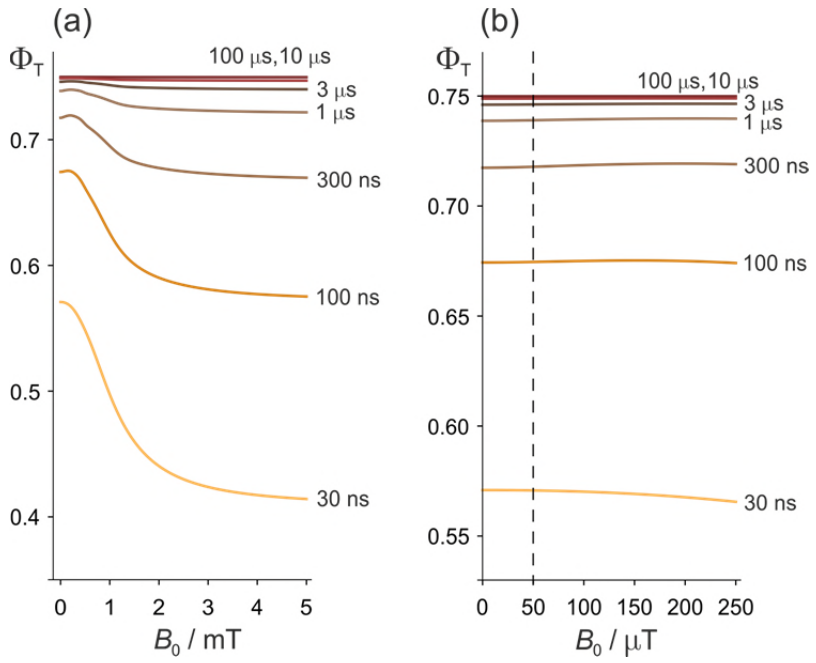

Figure 2–figure supplement 1. Effects of a static magnetic field on a model of the [FAD$^{\bullet-}$ TrpH$^{\bullet+}$] radical pair in cryptochrome. (a) Dependence of the reaction yield Φ_T on the static magnetic field strength, B_0, for different values of the radical pair lifetime, τ. The spin relaxation time is 0.1 μs. (b) An expanded view of the low field region of (a) with B_0 = 50 μT indicated by the dashed line.

bioRxiv preprint doi: https://doi.org/10.1101/502344; this version posted December 20, 2018. The copyright holder for this preprint (which was not certified by peer review) is the author/funder, who has granted bioRxiv a license to display the preprint in perpetuity. It is made available under aCC-BY 4.0 International license.

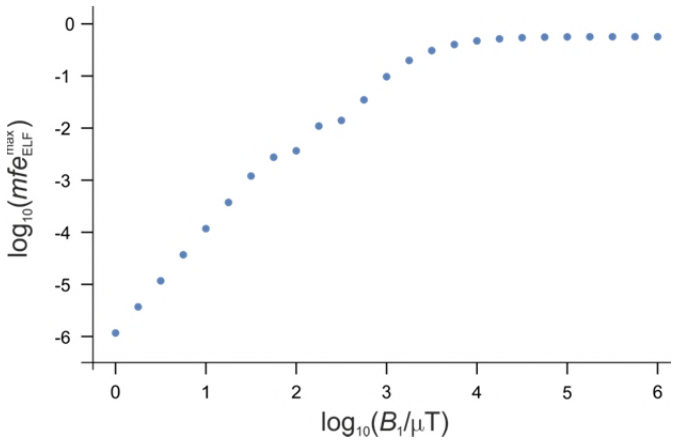

Figure 4–figure supplement 1. Dependence of $mfe_{\mathrm{ELF}}^{\max}$ on B_1 (1 μT ⩽ B_1 ⩽ 10^6 μT) for a model of the [$\mathrm{FAD}^{\bullet-}$ $\mathrm{TrpH}^{\bullet+}$] radical pair, with B_0 = 50 μT and r = 10^6 s^{-1}. mfe_{ELF} was evaluated by numerical integration of equation (4) over the phase α of the ELF field. The values of $mfe_{\mathrm{ELF}}^{\max}$ are all negative except for $\log_{10}(B_1/\mu\mathrm{T})$ = 2.00, 2.15, and 2.50. When $\log_{10}(B_1/\mu\mathrm{T}) \leq 1.5$, the gradient of this graph equals 2 as expected from equation (10).

bioRxiv preprint doi: https://doi.org/10.1101/502344; this version posted December 20, 2018. The copyright holder for this preprint (which was not certified by peer review) is the author/funder, who has granted bioRxiv a license to display the preprint in perpetuity. It is made available under aCC-BY 4.0 International license.

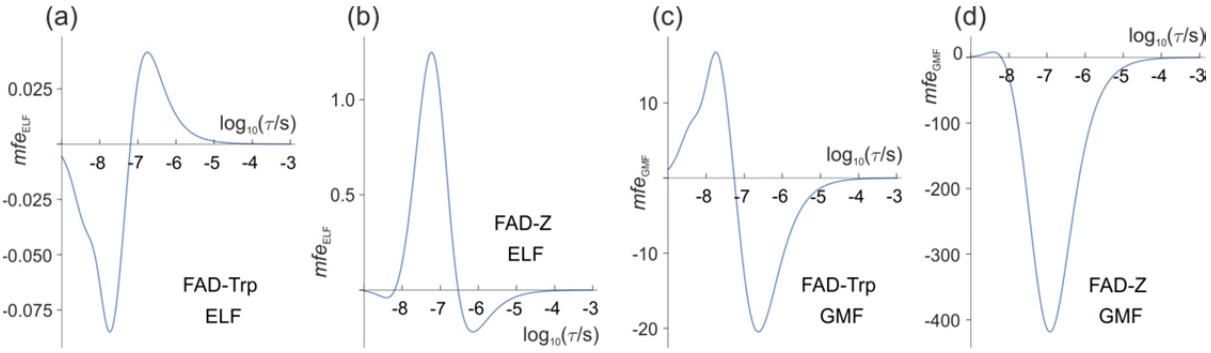

Figure 4–figure supplement 2. Magnetic field effects (in ppm) on model radical pairs as a function of the lifetime of the radical pair, τ, in the range 1 ns–1 ms. The spin relaxation time is 0.1 μs. (a) and (c) A model of the [$FAD^{\bullet-}$ $TrpH^{\bullet+}$] radical pair in cryptochrome, containing two ^{14}N nuclei in the $FAD^{\bullet-}$ radical and one in the $TrpH^{\bullet+}$ radical. (b) and (d) A model of the [$FAD^{\bullet-}$ $Z^{\bullet}$] radical pair in cryptochrome in which the $Z^{\bullet}$ radical has no hyperfine interactions. (a) and (b) mfe_{ELF} (equation (10)) for B_0 = 50 μT, B_1 = 1.0 μT. (c) and (d) mfe_{GMF} (equation (12)) for B_0 = 50 μT, ΔB_0 = –1.0 μT. Note the different vertical scales of the four panels. $mfe_{\mathrm{ELF}}^{\max}$ = –0.085 ppm for [$FAD^{\bullet-}$ $TrpH^{\bullet+}$] and +1.2 ppm for [$FAD^{\bullet-}$ $Z^{\bullet}$]. $mfe_{\mathrm{GMF}}^{\max}$ = –20 ppm for [$FAD^{\bullet-}$ $TrpH^{\bullet+}$] and –420 ppm for [$FAD^{\bullet-}$ $Z^{\bullet}$]. The corresponding values of $\Omega_{\mathrm{ELF}}^{\mathrm{GMF}}$ are 240 for [$FAD^{\bullet-}$ $TrpH^{\bullet+}$] and 350 for [$FAD^{\bullet-}$ $Z^{\bullet}$].

bioRxiv preprint doi: https://doi.org/10.1101/502344; this version posted December 20, 2018. The copyright holder for this preprint (which was not certified by peer review) is the author/funder, who has granted bioRxiv a license to display the preprint in perpetuity. It is made available under aCC-BY 4.0 International license.

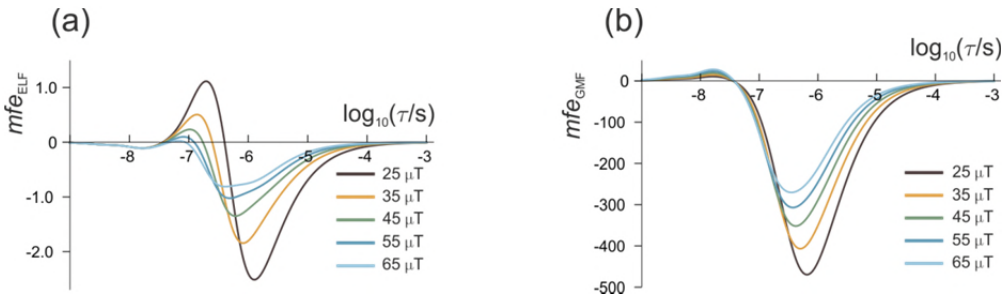

Figure 4–figure supplement 3. Magnetic field effects (in ppm) on a model of the [$FAD^{\bullet-}$ $TrpH^{\bullet+}$] radical pair as a function of the lifetime of the radical pair, τ, in the range 1 ns–1 ms for 25 μT ≤ B_0 ≤ 65 μT. (a) mfe_{ELF} and (b) mfe_{GMF}. B_1 = 1.0 μT, ΔB_0 = –1.0 μT, $r = 10^6$ s^{-1}. Note the different vertical scales of the two panels.